Optimised design of transverse-flux permanent-magnet synchronous generator with exterior rotor configuration used for renewable wind energy generation

Mahesh A. Patel

Published online: 04 Sep 2025.

Submit your article to this journal ↗

View related articles ↗

View Crossmark data ↗

Taylor & Francis
Taylor & Francis Group

Check for updates

Optimised design of transverse-flux permanent-magnet synchronous generator with exterior rotor configuration used for renewable wind energy generation

Mahesh A. Patel

Department of Electrical Engineering, Institute of Technology, Nirma University, Ahmedabad, India

ABSTRACT

The lack of conventional energy sources emphasises the penetration of renewable energy generation. Among all the renewable energy sources, wind power has the most potential to increase energy production needs. Different generators have been utilised for wind power generation, whereas in a transverse-flux permanent magnet generator, the exterior rotor concept offers better advantages than the inner rotor concept. In this paper, the design criteria and specifications are integrated by optimising the volume of the machine in comparison with the interior rotor configuration of TFPMGs. It deals with the determination of the design parameters of the proposed topology by means of a parameter sweep optimisation method. The dynamic (time-stepping), 3-D FE analysis has been carried out using the FEA tool to prove it a better topology for wind applications. The optimised parameters are validated through FE analysis.

1. Introduction

Various wind power generator concepts have been proposed with ample benefits as a result of the rapid advancement of wind power generator technologies and the improvement of installed capacity of wind power generation globally. The objective of the penetration is to reduce the cost of production of energy. Various futuristic generators for large wind power plants have been reviewed in Polinder et al. (2013) and the key benefits of direct-drive wind generator systems, i.e. increased overall efficiency, reduced maintenance, longer life, and availability due to the gearbox's omission – are highlighted when comparing DDPMG with geared-drive wind generator systems. A large comparison has been made in Chen (1998) and Li (2007), and low speed with higher number of poles are found to be best suitable as multi-pole permanent magnet generators (MPPMGs). The preliminary advantages of direct drive PM generators for higher rating wind power plants are depicted in Semken et al. (2012). Due to a greater power density and simple winding design, a conventional TFPMG with basic configuration of U-shaped core is explored in Gieras (2010), and Lange (1998), which is more suitable generator for direct-drive wind power plant. For increasing efficiency and lower the losses, various topologies have been modified and proposed in Dobzhanskyi, Mendrela, and Trzynadlowski (2011). The main disadvantages of a conventional TFPMGs are uneven magnetic flux distribution, large leakage fluxes, and complex design, due to magnets have been used during the process of energy conversion. To reduce the leakage flux, a part known as iron bridge is inserted between the stator cores, but this leakage induces an eddy current in it and hence reduces the overall flux linkages and that leads to greater power loss. A transverse-flux permanent-magnet generator with a new concept of fall-back rotor pole is presented in Patel and Vora (2017). An inner rotor design with fall-back

transverse-flux permanent-magnet generator (FB-TFPMG) (Patel and Vora 2020, 2023) includes elliptical stator core, toroidal coil and less number of permanent magnets in comparison with conventional TFPMG. The concept fall back path provides various benefits, i.e. it reduces the leakage losses in comparison with inactive magnets in conventional TFPMG and total cost of the machine.

The transverse flux PM generator with exterior rotor configurations are found in the literature (Kudrjavtsev et al. 2017; Mamur et al. 2020; Zarghani et al. 2024), stating various advantages, i.e. higher cooling surface area, less weight in comparison with conventional rotor configuration. To attain the goal of reduction in volume and weight at low speeds for direct coupling, the exterior rotor structure is analysed by Chen, Nayar, and Xu (1998). In Dobzhanskyi, Gouws, and Amiri (2016), transverse flux PM generator with exterior rotor designs are compared. The permanent magnet pole place could be changed for improved performance in permanent-magnet generators (PMGs) because of the space available in the exterior rotor design (Arafat et al. 2017). Various optimisation techniques (Dastani and Ardebili 2015; Lee et al. 2015; Polikarpova et al. 2015) have been explored to get the optimised parameters of permanent magnet generators.

In this paper, the study explores the prospect of improving the ratio of power-to-volume in comparison with the conventional FB-TFPMG by extending the new concept of FB-TFPMG to the exterior rotor design, which is appropriate for direct connection of wind turbines. The main objective of this research is to explore the feasibility of direct pairing of wind turbine blades to the exterior rotor to get the immediate benefits of cooling and less complex manufacturing process. The main benefit of the proposed configuration is that the outer periphery of the drum could be bolted with the blades of the wind turbine to obtain the straight coupling between them and that leads to

weight reduction and natural cooling. The novelty of the pro-posed fall-back topology utilises half of the permanent magnet as compared with the conventional topology of TFPMG, reduces the cost as well as the benefits due to outer rotor configu-ration. The construction and working principle of a proposed exterior rotor design of fall-back transverse flux PM generator (FB-TFPMG) are discussed briefly in Section 2. The design cri-teria and specifications have been presented in Section 3 with volume optimisation parameters. The parametric sweep method has been employed using 3-D finite element analysis to get the optimised parameters for the performance analysis. The results of magnetic field, and various plots under different conditions are tabulated in Section 4 and conclusion in Section 5.

2. An exterior rotor fall-back transverse-flux PM generator concept

2.1. Construction

The construction of a transverse flux permanent magnet genera-tor with fall-back exterior rotor (Patel and Vora 2020) is presented in Figure 1.

The FB-TFPMG is mainly a three-phase topology and its struc-ture is similar to the inner rotor topology, but rotor is arranged on the outer side. It utilises half of permanent magnets, as com-pared to the conventional TFPMG, essentially use the space in it, so that the PM rotor pole position can be modified for better per-formance to reduce cogging torque. An iron bridge is fixed over the fall-back rotor to restrict the leakage fluxes. One pole pair view of exterior rotor FB-TFPMG, with elliptical shaped U-stator core and iron bridge is shown in Figure 2.

The core assembly of the internal stator mainly consists of a number of stator cores (elliptical shape in cross-sectional) and is configured inside a rotor core assembly with an air gap. The stator core assembly is fastened with a fixed shaft. An elliptical U-stator core comprises iron material surrounding the toroidal stator coil. The stator coils are made of copper material and placed inside the stator cores. The back of the fall-back rotor is made of mild steel and the rotor contains the same number of PM rotor pole pairs as the number of cores in stator. The NdFeB magnetic material is used by the rotor PM poles. Inactive mag-nets are eliminated and the PM poles flux are transferred via fall-back rotor to effectively replace the inactive magnets. All
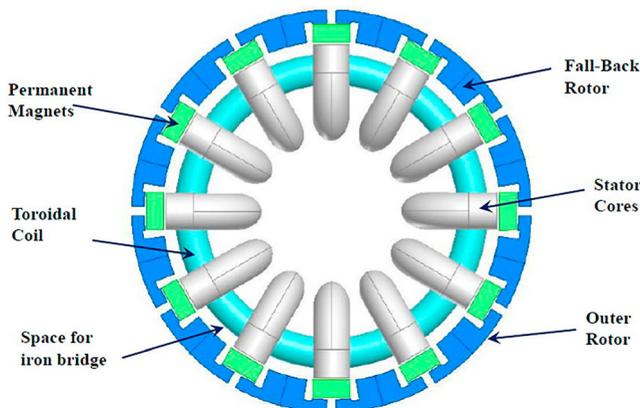

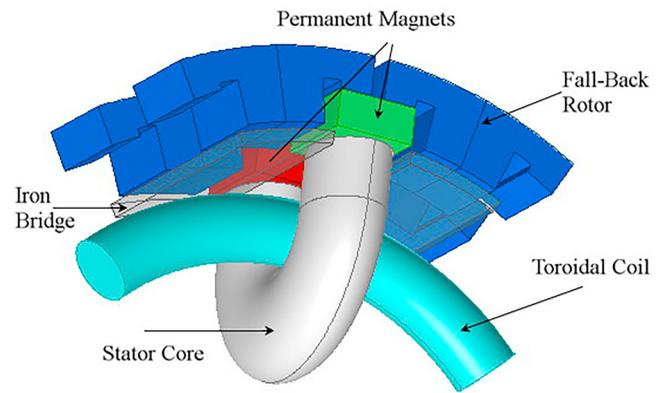**Figure 1.** Construction of Fall-back TFPMG.

Figure 2. One pole pair view of exterior rotor FB-TFPMG.

rotor PM poles are followed by a rotor fall-back part on the rotor surface. The magnetic fluxes originate inward to outward from all PM rotor poles from the front side and the flux originates out-ward to inward from all PM rotor poles from back-side PMs. The flux moves to the fall-back rotor part in a way that the flux direc-tion is opposite to that of the PM pole flux direction. The inner stator core flux direction is in the transverse direction. For the condition of rotor PM poles aligned with the stator core, the flux travels through a path, i.e. active PMs, air gap, stator core and iron bridge. The flux passes through the fall-back rotor part, air gap, stator U-core and iron bridge in an unaligned position. The exterior rotor topology is constructed with three magnetically independent phases, and comprises three separate stator and rotor units.

2.2. Working of FB-TFPMG with exterior rotor

The PM fluxes consistently add up to the stator core and after a rotation of rotor one pole pitch apart, the fluxes from the fall-back rotor add up to the stator core. As rotor rotates with respect to angular displacement, the PM rotor poles and fall-back rotor poles on the surface of the rotor change their position with respect to the stator core, an emf is induced in the stator winding. Maximum magnetic flux penetrates in one direction through the stator core and links to the stator coil, during the aligned condition between PM poles and stator core. Similarly, the flux passes in reverse direction during unaligned condition. The alternating induced emf with rotor position can be evalu-ated, if the number of turns per coil are known.

3. Design criteria and specifications

3.1. Design specifications

The first stage of developing a machine design is to formulate the design specifications as shown in Figures 3 and 4, with nomenclatures. where $D_{st,o}$ = the stator outer diameter, $D_{rt,o}$ = the rotor outer diameter, $D_{rt,i}$ = the rotor inner diameter, L_g = the length of air gap, H_u = the height of the stator core, (L_{pm} =)PM length, H_{pm} = PM height, W_{pm} = PM width, W_{fb} = the width of the fall − back part, H_{fb} = the height of the fall − back part, W_u = the width of stator core and D_{sc} = is the stator coil diameter.
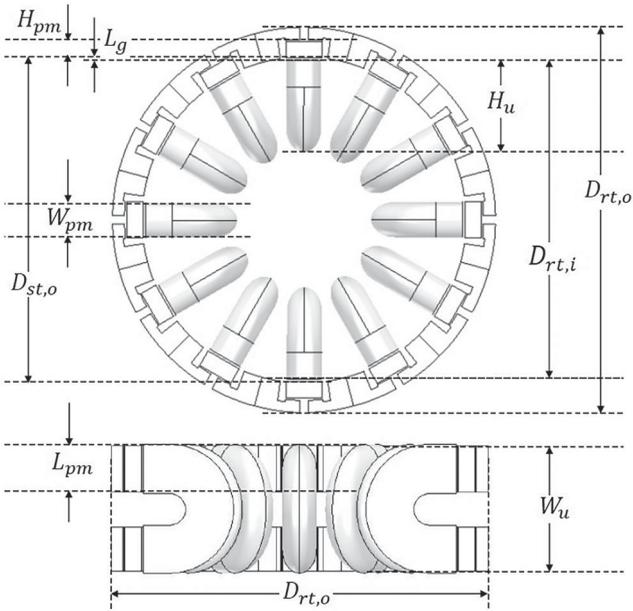
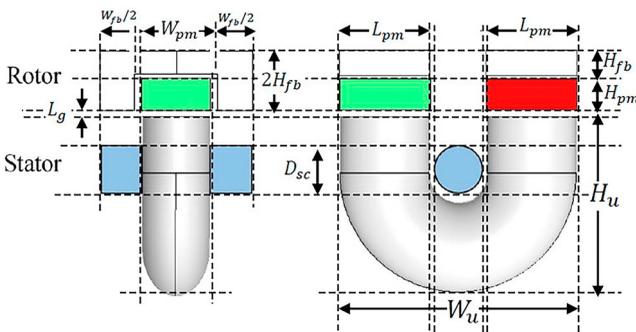**Figure 3.** Design dimensions of exterior rotor FB-TFPMG.

Figure 4. Design dimensions of one pole pair of exterior rotor FB-TFPMG.

To ensure higher efficiency at the operating speed of 300 rpm, a direct-drive FB-TFPMG topology with an exterior rotor is selected. The output power of the simulation prototype is set to 1 kW at 300 rpm. The maximum flux density in iron cores is considered as 1.1 T to avoid saturation, owing to increase in flux leakage which reduces the power factor. The FB-TFPMG with an exterior rotor configuration is a three-phase configuration with single coil in each section of the stator. For design criteria and simulation process, a single unit (single-phase) configuration is considered as depicted in Figure 5.

Each single phase configuration is made up of repeated sections over time intervals. Therefore, the design is limited to the single section for the purpose of design criteria. Based on the performance of a single section, the number of sections required to meet the performance of the machine is determined. The primary dimensions of the FB-TFPMG with exterior rotor are obtained from the design of the sections and the required number of sections as tabulated in Table 3.

The goal of optimisation is to acquire the FB-TFPMG design with a high power to volume ratio by satisfying the constraints in comparison with the interior rotor FB-TFPMG. For step-by-step
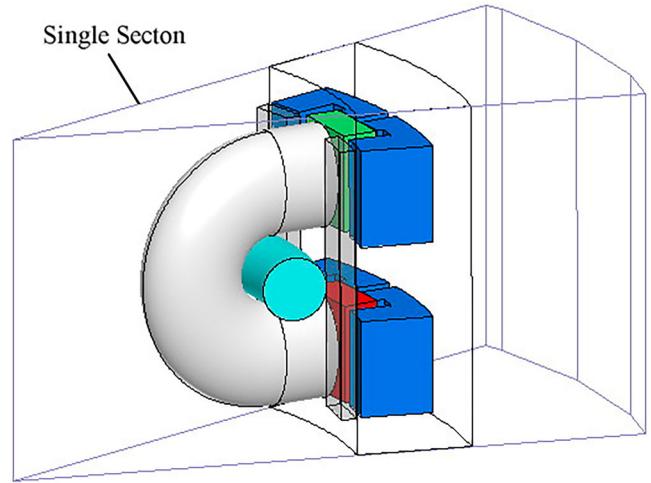

Figure 5. Cut section for FE analysis of exterior rotor FB-TFPMG.

Table 1. Parameter range during parameter sweep.

Parameter (mm)	Range	Step size
H_{pm}	5–8	0.2
W_{pm}	9–20	1
L_{pm}	9–20	1
D_{sc}	3–15	1

procedure to obtain a design of FB-TFPMG sections, the fulfilment of the requirement starts by calculating the flux of the magnet and coil flux. The flux through air gap and through a core is calculated by air-gap flux density. It can be assumed that the flux passes through the core, as this path has very low reluctance than any other path through air. Integrating flux density under one stator leg results in similar flux passing through the side of the core of FB-TFPMG. The corresponding flux linkage of the coil due to the flux of permanent magnet can be computed, by varying the magnet dimensions of the FB-TFPMG in the range selected for a parameter sweep as tabulated in Table 1. The electric current loading in the coil, corresponding to flux linkages can be determined. The reluctance of the coil of FB-TFPMG is calculated from the parameter sweep over the magnet array dimensions. With the obtained reluctance and maximum allowable flux, the MMF can be calculated. Using the total MMF required and the specified current density, the dimension of the coil is calculated.

After obtaining, the dimensions of the permanent magnet and the stator coil, the FBTFPMG section and the required number of sections are determined and finally the dimensions of the whole FB-TFPMG machine. The machine design that satisfies the constraint has been checked for constraints of inner rotor FB-TFPMG. Finally, the machine design with the lowest total volume which satisfies the constraints imposed can be selected from the designs obtained by the parameter sweep method.

3.2. Design criteria for volume optimisation

The volume optimisation of the exterior rotor FB-TFPMG is analysed with the help of parameter sweep of different important key parameters as shown in Table 1. The magnet height H_{pm}, width W_{pm} and length L_{pm} decide main dimensions of the
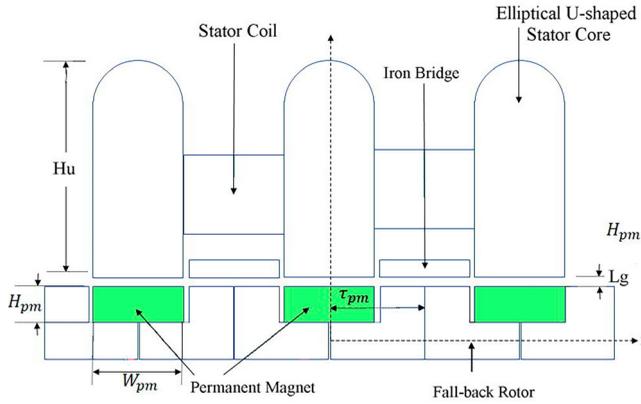
Figure 6. Permanent magnet positions of exterior rotor FB-TFPMG.

Table 2. Dimensions of different cases of exterior rotor FB-TFPMG.

Parameters (mm)	I	II	III	IV
Outer diameter of rotor	146	168	170	171
Inner diameter of rotor	121	140	141	141
Average diameter of the air-gap	120	139	140	140
Stator exterior diameter	119	138	139	139
Width of fall-back part	13.6	15.7	16	16.1
Height of PM	6.82	7.1	7.2	7.28
Length of PM	17	19	19.5	20
Width of PM	13.59	15.7	15.9	15.9
Axial width of the Generator	46.9	54	53.8	55

Table 3. Design dimensions of FB-TFPMG with exterior rotor.

Parameters	Dimensions (in mm)
Outer diameter of the rotor	170
Inner diameter of the rotor	141
Outer diameter of the stator	139
Average diameter of the air-gap	140
Width of the Fall-back part	16
Axial length of generator	53.8
Air-gap flux density	1.2 T
Total PM plus fall-back rotor poles	24
Stator U-cores	12
Number of turns per coil	24
Speed of the rotor	300 rpm
PM length (L_{pm})	19.5
PM height (H_{pm})	7.2
PM width (W_{pm})	16
Relative permeability of NdFeB magnet	1.0596 H/m

machine. The other key parameter is coil dimension (diameter of the coil D_{sc}). The magnet pole pitch (τ_{pm}) and magnet height H_{pm} are the parameters that determine the main flux path over a cross-sectional area of the permanent magnet and the stator leg, and is proportional to the flux crossing the air gap as shown in Figure 6.

The length of the magnet decides the length of the iron bridge. Hence the magnet length is proportional to two of the four leakage flux paths. If the magnet length is increased, the overall axial length of the generator is also proportionally increased. The minimum machine volume according to the requirement of the air-gap flux density is achieved by changing the length of the magnet. The length of the magnet can be reduced with respect to its width of the magnet to get the less leakage flux. The magnet width W_{pm} is the other parameter of the two parameters that determines the cross-sectional area of the permanent magnet and main magnetic flux in the air gap. Furthermore, it is proportional and related to two leakage permeance, i.e.the direct inner pole leakage permeance and inner core leakage permeance. The dominating leakage path is the inner core leakage path, as the gap between the permanent magnets is small compared to the dimensions of the coil. Thus the leakage paths are dependent of the magnet width and a small influence on the flux due to the current. The height of the permanent magnet H_{pm} leads to increase flux density in air gap, up to a certain extent. If the height of the permanent magnet increases, the reluctance is also increased proportionally, due to low permeability of the permanent magnets. The limitation of increasing the value of height of PM (H_{pm}) is due to the saturation of the core and the overall dimensions would affect by increasing the height of the magnet. Thus the increment in height beyond the values of the parameter sweep may result in further reduction of the machine volume. The permanent magnet height is restricted between 5 H_{pm} 8 mm. The lower magnet height boundary is chosen such that the magnet might be partially demagnetised, where the increase in height of magnet beyond the upper limit would result in higher air-gap flux density at considerably higher material cost. The magnetic flux of PM increases for a fixed ratio between the magnet length and the magnet gap. However, for small pole pitches the inter pole leakage is increased, which reduces the magnetic flux. The radial gap is the space between two consecutive rotor poles, i.e. it is the pole pitch minus the magnet width. If the space

between two magnets is larger, it may suffer from less inter pole leakages and air-gap flux increases somewhat. This allows for a reduction in the magnetic material in a pole pitch without spoiling the performance of the machine. The coil dimensions determine its MMF of the coil in combination with the assumed current density. The coil diameter directly influences the axial length of the machine and the inter pole leakage permeance of the stator. An increase in the coil diameter, resulting in an equal increase in axial length, results in a severe penalty on the generator volume and torque density. The diameter of the coil is selected as the driven dimension, as this parameter does not have any influence on the size of the air gap and flux distribution in the air gap due to the magnets. It can be varied without influence on the flux due to permanent magnets and selected depending upon the required power factor. The power factor of FB-TFPMG depends on the ratio of magnetic flux and coil flux. Hence, one of the key parameters is a driven dimension depending on the power factor and the other is the torque density.

3.3. Parameter sweep method for o ptimisation

The performance parameters of the exterior rotor FB-TFPMG are calculated over a four-dimensional parameter sweep, of which three parameters belong to the magnet array and one to the coil. These four parameters of the sweep are listed in Table 1 with their corresponding values.

3-D FE analysis has been carried out using the parameter sweep values and four different cases have been observed as mentioned in Table 2 to obtain an equal output of the machine compared with the inner rotor FB-TFPMG.
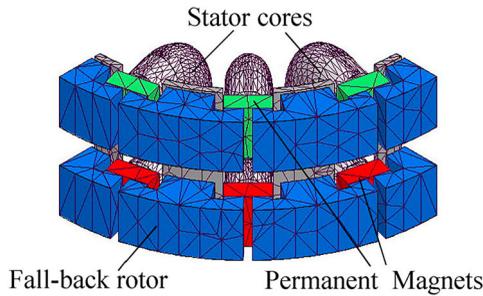
Figure 7. The meshing plot of the exterior rotor FB-TFPMG.

Figure 8. Flux density vector plot of exterior rotor FB-TFPMG.

In the first case, the air-gap diameter of both the configurations is maintained the same. In the second, third and fourth cases of the exterior rotor FB-TFPMG, the exterior diameter is kept smaller than the case of inner rotor FB-TFPMG and the axial height of the generator is larger than the conventional one. It has been observed that, in the third case where, output power of both the inner and exterior rotor configuration is observed similar with the reduction in volume with exterior rotor configuration. The design of the full machine is based on the parameters of the design with the lowest machine volume for a magnet height of $H_{pm} = 7.2$ mm. For the same power output, reduction in volume is achieved by finalizing the parameters as shown in Table 3.

4. Results and d iscussion

4.1. 3-D FE analysis of exterior rotor FB-TFPMG

A magneto-static and 3-D transient (time-stepping)finite element analyses (FEA) of the exterior rotor FB-TFPMG have been carried out, suitable for low speed direct-drive wind power plants at no load. The final dimensions of the exterior rotor FB-TFPMG, obtained from the previous sections as tabulated in Table 3, are used for the analysis after analysing different design configurations and optimizing the parameter sweep method. NdFeB permanent magnets are selected for the analysis. The meshing plot of the exterior rotor FB-TFPMG model is depicted in Figure 7.

The model was meshed using a first-order mesh with 29,711 tetrahedral elements. The mesh size used in the FEA is controlled and optimised to achieve good quality meshing while deciding the simulation time. Each design iteration in the FEA domain took approximately 215 seconds. Solving the model with a second-order mesh drastically increases the FEA simulation time from 3.5 to 30 minutes. For initial sizing of the machine, which requires multiple design iterations, the second-order mesh can be used for accurate result analysis.

A static analysis of a single section geometry is analysed using 3-D FEA to find the flux distribution in the air gap, rotor and stator parts of the exterior rotor. The mmf of the PM is the major source of the fluxes in the air gap and passes through the stator core and links to the stator coils. Simultaneously, the fluxes flow in the fall-back rotor part in reverse direction. During an aligned condition of rotor PM poles, fall-back rotor and U-stator core, a flux density vector plot of FB-TFPMG with exterior rotor configuration is presented in Figure 8.
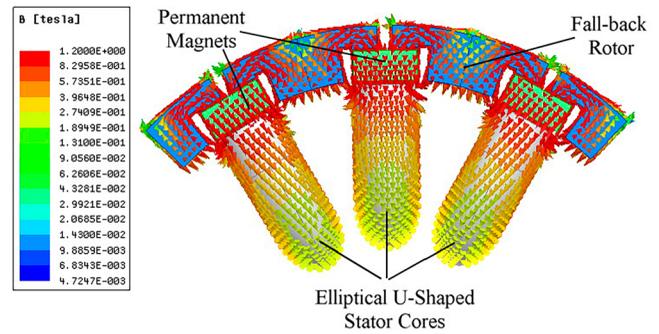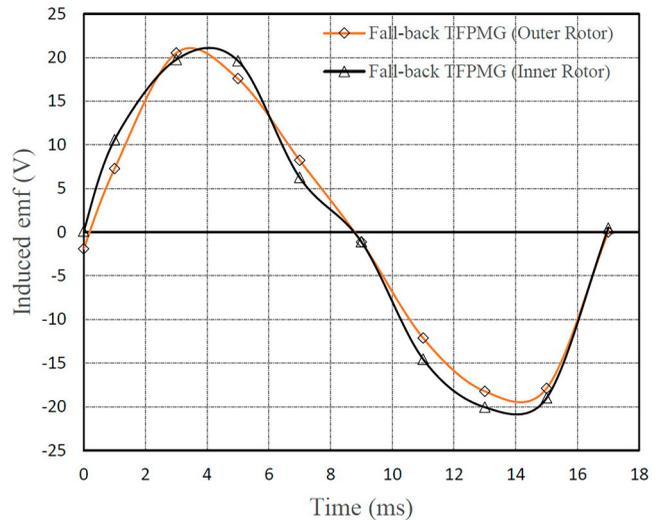

Figure 9. Induced emf under no load condition of FB-TFPMGs.

4.2. No load and on load induced emf of FB-TFPMGs

An exterior rotor FB-TFPMG has been analysed through 3-D transient (time-stepping) FE analysis under no-load condition. The design specifications for the analysis of a prototype simulation are tabulated in Table 3. Master and slave boundary conditions are applied for the analysis. A single section of one phase is used for the analysis, due to three independent phases, neglecting the eddy current effect. The no-load induced emf plot is depicted in Figure 9. Two different topologies are evaluated, i.e. inner and exterior rotor FB-TFPMG and their induced emf under no-load condition are compared.

Transient analysis has been carried out for different speeds ranging from 50 to 600 rpm to check the low speed characteristics of the exterior rotor FB-TFPMG for direct-drive wind power generator, which operates at low speed. Figure 10 shows the induced emf under no load with different speed ranges.

The dimensions and specifications of inner rotor FB-TFPMG of single unit have been considered from Patel and Vora (2020) for comparison with exterior rotor FB-TFPMG. FE analysis under loading condition of the FB-TFPMG with exterior rotor is carried out by connecting a 1kW, R-L load to the generator with the impedance of 3.41 ohm per phase to its terminal, and results are compared in Figure 11.
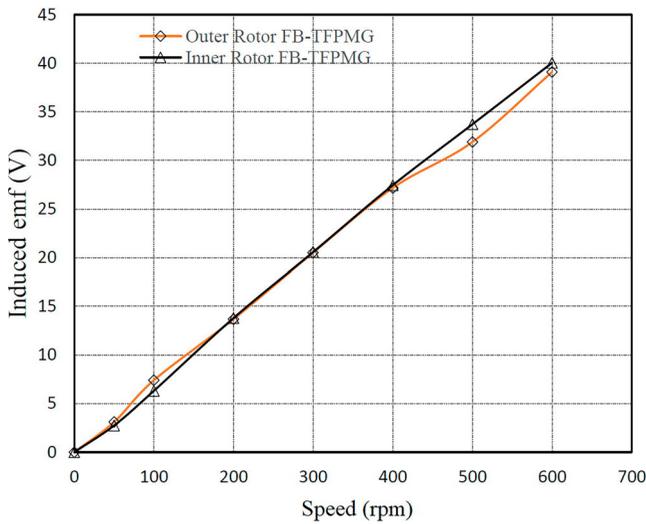
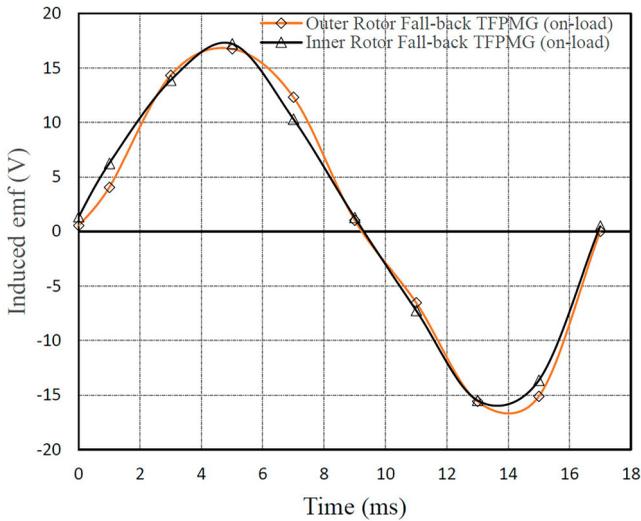**Figure 10.** Induced emf versus speed plot of FB-TFPMG.

Figure 11. Induced emf under loading condition of FB-TFPMG.

Figure 12. Comparison of torque of both FB-TFPMG topologies.
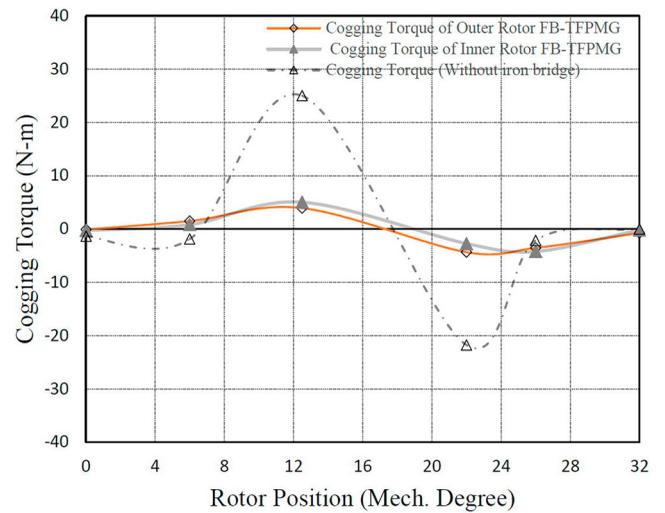
Figure 13. Cogging torque analysis of both FB-TFPMG topologies.

The electromagnetic torque plot has been compared for both inner as well as exterior rotors of FB-TFPMG topologies as shown in Figure 12.

In conventional TFPM generator, the cogging torque is observed higher due to its transverse flux structure. The cogging torque phenomenon is due to the interaction between variable permeance of the air gap due to the stator pole teeth and the rotor PM pole. To get an optimal generator design, the cogging torque should be minimised. In proposed configuration, due to fall-back rotor path, the distance between two PMs has increased the reduction in cogging torque. Cogging torque under loading conditions of inner rotor FB-TFPMG and exterior rotor FB-TFPMG with iron bridge and exterior rotor FB-TFPMG without iron bridge have been compared in Figure 13.

The PM generator topology is compared with respect to volumes, while producing equal power output under loading condition. Due to the size constraints in the Nacelle, which is an outer cover for wind turbine assembly, the generator diameter should not be increased beyond the limitation. The gross diameter of the FB-TFPMG with external rotor measured 170 mm after
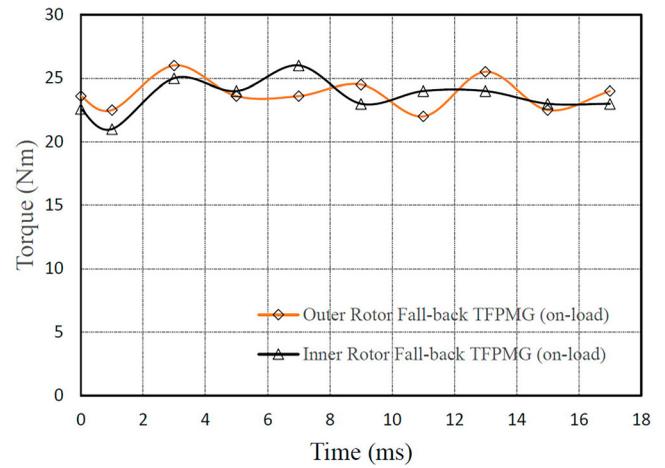
optimisation, whereas the diameter of inner rotor is measured 192 mm in Patel and Vora (2017). The axial length measured with exterior rotor FB-TFPMG is 53.8 mm and with FB-TFPMG with inner rotor is 47 mm. The overall volume of the FB-TFPMG with exterior rotor is reduced by 10.27 percent compared with the inner rotor, by reducing the overall diameter by 11.45 percent and increasing the height by 14.46 percent.

5. Conclusion

The fall-back exterior rotor concept of FB-TFPMG and its functioning have been described in detail with their benefits. In comparison with inner rotor topology, exterior rotor FB-TFPMG was optimised through a parameter sweep method and the effects of dimensions of permanent magnets on the performance of machine have been discussed in depth. Optimised dimensions of the exterior rotor FB-TFPMG were obtained to analyse the output parameters in comparison with the inner rotor topology. To maximise power to volume ratio of the FB-TFPMG, it has been analysed using FEA tool. The static analysis was performed to observe the flux distribution in the fall-back rotor, stator and air gap. Through time-stepping 3-D FE analysis, an induced emf

under loading conditions were obtained and compared with the inner rotor topology. After applying a parameter sweep optimisation technique, a reduction in volume of 10.27 percent is gained when compared with conventional rotor topology and gives the equivalent output power as compared with the inner rotor design to improve power-to-volume ratio. The contribution of this research is to get the optimised volume and benefits to better cooling due to exterior rotor and the less cost due to half the permanent magnet utilisation of the improved FB-TFPM generator. The new exterior rotor concept of FB-TFPMG is further economically attainable for application to direct-drive wind generation technology.

Future scope

The author has analysed the 3-D electromagnetic time stepping analysis of the exterior rotor FB-TFPMG using FEA tool. Further, author suggests to the research community to carry out the thermal analysis using FEA tool to predict the thermal losses due to the generation of heat and the effect of permanent magnet demagnetisation of FB-TFPMG. It could help to improve the accuracy of the prediction of generator performance. Structural analysis of the proposed topology needs to be performed using FEA tool to optimise the dimensions of the machine without sacrificing the deformation of the novel topology of exterior rotor FB-TFPMG.

Author contributions

CRediT: **Mahesh A. Patel:** Investigation, Methodology

Disclosure statement

No potential conflict of interest was reported by the author(s).

Data availability statement

The data that support the findings of this paper are available from the corresponding author upon reasonable request.

ORCID

Mahesh A. Patel http://orcid.org/0000-0003-0342-0038

References

Arafat, Y., M. Murshed, M. Hasan, and M. A. Razzak. 2017. "Design and Performance Analysis of a Modified Outer Rotor Permanent Magnet Alternator for Low- Speed Wind Turbine." In *Proceedings of 9th International Conference on Electrical and Computer Engineering, ICECE*, Dhaka, Bangladesh, 2016, 511–514.

Chen, J. Y. 1998. "Design and FE Analysis of an Outer- Rotor PM Generator for Directly- Coupled Wind Turbine Applications." In *Conference Record of 1998 IEEE Industry Applications Conference, Thirty-Third IAS Annual Meeting*, St. Louis, MO, USA, 1998, 387–394.

Chen, J. Y., C. Nayar, and L. Xu. 1998. "Design and Fe Analysis of an Outer- Rotor Pm Generator for Directly- Coupled Wind Turbine Applications." In *Conference Record of 1998 IEEE Industry Applications Conference. Thirty-Third IAS Annual Meeting (Cat. No.98CH36242)*, St. Louis, MO, USA, 1998, Vol. 1, 387–394.

Dastani, M., and M. Ardebili. 2015. "Optimal Design and Analysis Simulation of an Outer Rotor Hybrid Excited Generator for Wind Energy Conversion Systems." In *ICEE 2015 – Proceedings of the 23rd Iranian Conference on Electrical Engineering*, Tehran, Iran, 2015, 1474–1479.

Dobzhanskyi, O., R. Gouws, and E. Amiri. 2016. "Comparison Analysis of Pm Transverse Flux Outer Rotor Machines with and without Magnetic Shunts." In *2016 IEEE Energy Conversion Congress and Exposition (ECCE)*, Milwaukee, WI, USA, 2016, 1–8.

Dobzhanskyi, O., E. E. Mendrela, and A. M. Trzynadlowski. 2011. "Analysis of Leakage Flux Losses in the Transverse Flux Permanent Magnet Generator." In *2011 IEEE Green Technologies Conference*, Green, Baton Rouge, LA, USA, 2011, 1–6.

Gieras, Jacek F. 2010. "Transverse Flux Machine," Patent US 7,830,057 B2.

Kudrjavtsev, O., T. Vaimann, A. Kilk, and A. Kallaste. 2017.Design and prototyping of outer rotor permanent magnet generator for small scale wind turbines,"*2017 18th International Scientific Conference on Electric Power Engineering (EPE)*, Kouty nad Desnou, Czech Republic, 2017, pp. 1–6. https://doi.org/10.1109/EPE.2017.7967237.

Lange, A. 1998. "Transverse Flux Machine," Patent US 5,773,910.

Lee, J. H., J.-Y. Song, J.-W. Kim, Y.-J. Kim, and S.-Y. Jung. 2015. "Optimal Design of Outer- Rotor Spmsg for Permanent Magnet Reduction Using Optimization Method." In *2015 18th International Conference on Electrical Machines and Systems (ICEMS)*, Pattaya, Thailand, 93–97.

Li, Z. C. H. 2007. "Overview of Different Wind Generator Systems and Their Comparisons." *Renewable Power Generation, IET* 2 (2): 123–138. https://doi.org/10.1049/iet-rpg:20070044.

Mamur, H., C. Şahin, M. Karaçor, and M. R. A. Bhuiyan. 2020. "Design and Fabrication of an Outer Rotor Permanent Magnet Synchronous Generator with Fractional Winding for Micro-wind Turbines." *IET Electric Power Applications* 14 (12): 2273–2282. https://doi.org/10.1049/elp2.v14.12.

Patel, M. A., and S. C. Vora. 2017. "Analysis of a Fall- Back Transverse- Flux Permanent- Magnet Generator." *IEEE Transactions on Magnetics* 53 (11): 1–5. https://doi.org/10.1109/TMAG.2017.2702745.

Patel, M. A., and S. C. Vora. 2020. "Analysis of a Transverse Flux Permanent Magnet Generator with Fall- Back Outer Rotor Design for Wind Power Generation." *International Journal of Ambient Energy* 41 (11): 1308–1313. https://doi.org/10.1080/01430750.2018.1507948.

Patel, M. A., and S. C. Vora. 2023. "Analytical Performance Estimation of a Fall-Back Inner- Rotor Transverse- Flux Permanent Magnet Generator Using Magnetic Equivalent Reluctance Circuit." *Electric Power Components and Systems* 51 (8): 733–745. https://doi.org/10.1080/15325008.2023.2180694.

Polikarpova, M., P. Ponomarev, P. Röyttä, S. Semken, Y. Alexandrova, and J. Pyrhönen. 2015. "Direct Liquid Cooling for an Outer- Rotor Direct-Drive Permanent- Magnet Synchronous Generator for Wind Farm Applications." *IET Electric Power Applications* 9 (8): 523–532. https://doi.org/10.1049/elp2.v9.8.

Polinder, H., J. A. Ferreira, B. B. Jensen, A. B. Abrahamsen, K. Atallah, and R. A. McMahon. 2013. "Trends in Wind Turbine Generator Systems." *IEEE Journal of Emerging and Selected Topics in Power Electronics* 1 (3): 174–185. https://doi.org/10.1109/JESTPE.2013.2280428.

Semken, S., M. Polikarpova, P. Roytta, J. Alexandrova, J. Pyrhönen, J. Nerg, A. Mikkola, and J. Backman. 2012. "Direct- Drive Permanent Magnet Generators for High- Power Wind Turbines: Benefits and Limiting Factors." *Renewable Power Generation, IET* 6:1–8. https://doi.org/10.1049/iet-rpg.2010.0191.

Zarghani, A., M. Farahzadi, A. Ghaheri, and K. Abbaszadeh. 2024. "Accurate 3D Thermal Network Development for Direct- Drive Outer- Rotor Hybrid-Pm Flux- Switching Generator." *Chinese Journal of Electrical Engineering* 10 (2): 80–92. https://doi.org/10.23919/CJEE.2024.000059.